buildings

MDPI

Article

Study on the Modified Ventilation Network on the Ventilation Effect and Ozone Migration Characteristics in Grain Pile

Kaimin Yang, Fengjiao Chu, Jiabin Li, Yuancheng Wang, Xiaoqian Dong, Jiying Liu and Yudong Mao *

School of Thermal Engineering, Shandong Jianzhu University, Jinan 250101, China; yangkaimin@sdjzu.edu.cn (K.Y.); jxl83@sdjzu.edu.cn (J.L.)
* Correspondence: maoyudong@sdjzu.edu.cn

Abstract: Grain is an important material for human survival. However, the expanding world population is contributing to a growing grain shortage. In order to reduce the loss of grain due to pests and mold during storage, mechanical ventilation as the main method of ventilation has crucial research significance. This article proposed and analyzed the ventilation effect and the migration characteristics of ozone in the grain pile under the modified ventilation network (MVN) and compared it with the original ventilation network (OVN). The study found that the temperature, moisture, and ozone concentration in the grain pile of the two ventilation networks are not evenly distributed in the vertical direction, showing a layered pattern. That is, with an increase in grain stack height, the temperature and moisture content of the grain stack are higher, and the ozone concentration is lower. Moreover, in the pre-ventilation period, the average temperature decline rate of the MVN was 1.25 °C/d, which was better than that of the OVN (0.84 °C/d), and the maximum temperature difference between the MVN and the OVN was 0.89 °C. The vertical ducts added to the MVN improved the ventilation effect, maintaining high ozone concentrations within the grain pile. Notably, on the sixth day of fumigation, the average ozone concentration of the MVN exceeded that of the OVN. The MVN can solve the shortcomings of the OVN, where air intake and fumigation gas rise slowly in the vertical direction. These findings hold substantial significance for optimizing ventilation network structures, devising effective fumigation strategies, and enhancing the insecticidal effects of grain storage.

Keywords: air ducts; heat and moisture transfer; ozone fumigation; migration patterns

Citation: Yang, K.; Chu, F.; Li, J.; Wang, Y.; Dong, X.; Liu, J.; Mao, Y. Study on the Modified Ventilation Network on the Ventilation Effect and Ozone Migration Characteristics in Grain Pile. *Buildings* **2024**, *14*, 604. https://doi.org/10.3390/buildings14030604

Academic Editor: Eusébio Z.E. Conceição

Received: 15 January 2024
Revised: 8 February 2024
Accepted: 21 February 2024
Published: 24 February 2024

1. Introduction

Grain plays a pivotal role in ensuring people's well-being and enhancing their quality of life. Nevertheless, as the global grain supply tightens and grain prices continue to rise, the issue of grain security must not be underestimated [1]. In sub-Saharan Africa, post-production food losses account for approximately 25 percent, with an estimated value exceeding one billion dollars [2]. The primary culprits behind these substantial losses in grain storage are inadequate storage facilities and suboptimal management practices [3]. As a result, there is an urgent necessity to implement effective measures aimed at safeguarding food security and mitigating post-production storage losses [4].

Storehouses constitute the predominant form of grain storage, and employing mechanical ventilation stands as a critical method for maintaining the temperature and moisture levels within safe storage limits for the grain pile stored in the storehouse [5]. Meanwhile, the ventilation network plays a pivotal role in facilitating this process within the grain pile [6]. According to the different arrangements of the ventilation ducts on the ground, they can be divided into U-shaped, F-shaped, and so on. The U-shaped ventilation network tends to create ventilation dead zones near the walls, leading to inadequate air circulation. Although the F-shaped ventilation network resolves the uniformity issues, it arranges the ground cage differently, resulting in a slower upward movement of incoming air vertically.

While phosphine fumigation is a common method employed to control pests in grain storage, its effectiveness has been limited by the growing resistance of insects to the original phosphine fumigant [7]. In response to this challenge, numerous studies have highlighted the substantial advantages of using ozone for managing grain storage insects and bacteria, presenting it as a promising alternative to phosphine [8]. However, during the fumigation process, if ozone gas is not fully dispersed in the grain pile, its effectiveness in sterilizing and eradicating insects will be affected [9].

Hammami et al. [10] developed a mathematical model centered on heat transfer within cylindrical grain silos during aeration. Chen et al. [11] carried out experimental and numerical studies to study the advantages of the double-skin roof for grain depots and the effect of physical parameters on convective heat transfer. Wang et al. [12,13] delved into the organization of airflow and the distribution of heat and moisture transfer, combining numerical simulations with experimental validation, within different types of grain storage facilities. Thorpe et al. [14] conducted an in-depth investigation into the heat transfer, mass transfer, and moisture transfer processes within grain piles. Their equation accurately represents the heat and moisture transfer phenomena in grain piles. Bonjour et al. [15] undertook experiments related to fumigation and insecticide treatments in experimental silos, varying ozone concentrations. Wang et al. [16] studied the transport properties of gaseous ozone in soil. Silva et al. [17,18] utilized CFD to calculate chemical degradation constants and effective diffusion coefficients for ozone gas as it permeated rice grains. They also established controlling equations governing the transport of ozone components within grains.

In summary, great progress has been made in the study of grain piles, but much of the existing research has been limited to a specific ventilation network. For the optimization of ventilation networks, most of the focus is on redesigning the pipe layout, without considering adding pipes in the vertical direction to obtain better ventilation effect. Concerning fumigation, prior research has primarily focused on evaluating the effectiveness of ozone in preventing pests in stored grains; however, the study of ozone migration patterns was lacking. Moreover, numerical simulation technology has been used skillfully in the study of ventilation.

To address this issue, this article has proposed a modified ventilation network (MVN). The MVN has modified the original F-shaped ventilation network (OVN) by adding vertical ducts to the above-ground ventilation ducts. Moreover, to prove that the modification is effective, this paper employed numerical simulation to analyze the ventilation effects and ozone migration characteristics within grain piles under the modified ventilation network, comparing it with the OVN. The ventilation effects were analyzed from the perspectives of temperature and moisture, and the ozone migration characteristics were analyzed from the dimensions of time, grain layer, and particle adsorption. In addition, by adjusting the inlet ozone concentration during fumigation, an in-depth analysis was conducted on whether the ozone migration characteristics change with different concentrations. This study provides valuable insights for selecting the optimal ventilation network based on the storage capacity of the storehouse. It has important significance in enhancing the fumigation process and improving various aspects of grain storage management. Optimizing the ventilation network helps to improve the uniformity of air flow and avoid the formation of hot spots in the accumulation of grains, thereby reducing mass loss. It provides a more even gas distribution during fumigation. This helps to ensure that the fumigant reaches the entire storage area, thereby increasing the insecticidal effectiveness of the fumigant.

2. Materials and Methods

2.1. Physical Model

In this study, we developed a physical model based on actual storehouse dimensions. The storehouse has a width of 22.86 m, a length of 37.22 m, and a height of 10.5 m (X = 22.86 m, Y = 37.22 m, Z = 10.5 m). The grain is stacked to a depth of 6 m, with a total grain storage capacity of 3959 t. The storehouse employs a two-way ventilation system,

featuring eight inlets and twelve exit windows. To prevent the formation of ventilation dead zones, the windows on the sides are distanced from the mountain wall by 1 m, as shown in Figure 1.

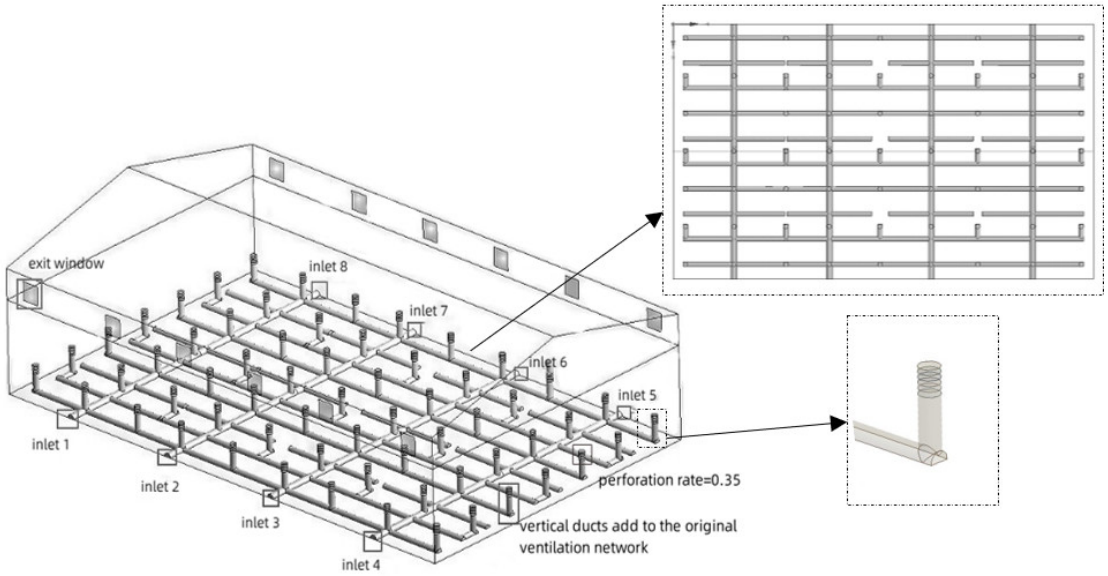

Figure 1. Physical model of the MVN.

The OVN comprises main ducts with a diameter of 0.5 m and branch ducts with a diameter of 0.4 m. In the MVN, vertical ducts with a diameter of 0.4 m were introduced to the OVN, as shown in Figure 2. To ensure even and efficient ventilation, these vertical ducts were evenly distributed within the grain pile. The vertical ducts are spaced at intervals of 4.3 m with a span interval of 3.4 m. Each vertical duct has a height of 1.5 m and a percent opening of 35%. At intervals of 0.1 m, independent control units were installed, allowing for subsequent simulation and analysis of the effects of varying vertical duct heights on grain pile ventilation.

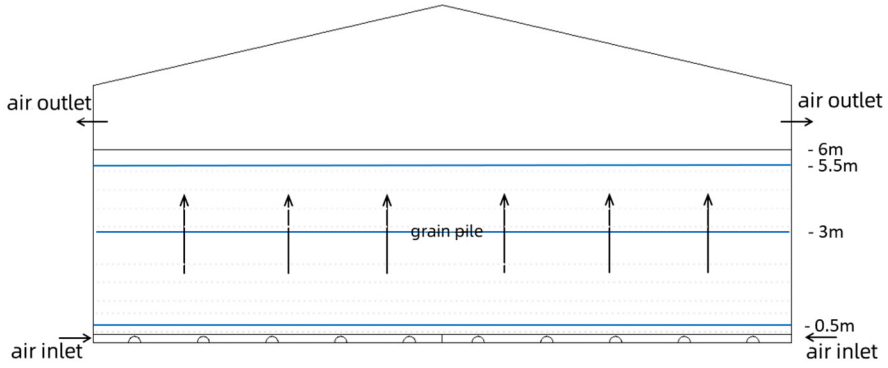

(**a**)

Figure 2. *Cont.*

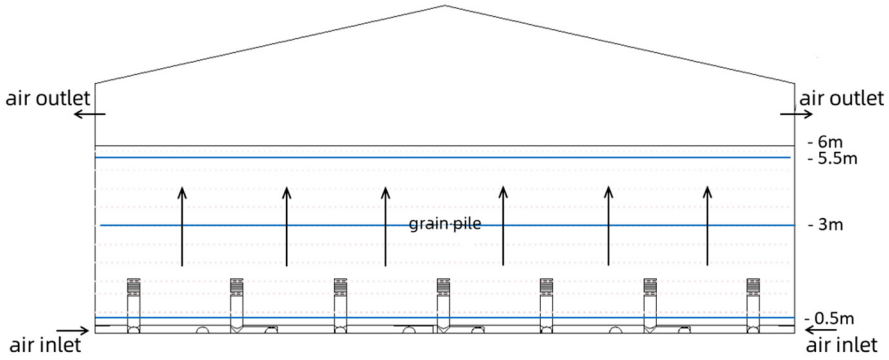

(**b**)

Figure 2. Side view of the two ventilation networks. (**a**) The OVN; (**b**) the MVN.

2.2. Mathematical Model

The grain pile consists of grains piled up, there are gaps between the grains, and the gaps are filled with air; so, the pile can be regarded as a porous medium [19]. The continuity equation within the grain pile is the following:

$$\varepsilon_a \frac{\partial \rho_a}{\partial t} + \nabla \cdot (\rho_a u) = 0 \tag{1}$$

where ε_a is the porosity of the grain pile; ρ_a is the air density, in kg/m^3; u is the gas velocity, in m/s; and ∇ is the Hamiltonian operator.

For a porous medium such as a grain pile, the enthalpies of the gaseous and solid phases are considered, so the heat transfer equation within the pile can be expressed as follows:

$$\rho_b c_b \frac{\partial T}{\partial t} + c_a \nabla \cdot \left(\rho_a \vec{u} T\right) = k_{eff} \nabla^2 T + h_{fg}(1-\varepsilon_a)\rho_b \frac{\partial W_w}{\partial t} \tag{2}$$

where c_a and c_b are the specific heat of air and grain, respectively, in J/(kg·K); W_w is the moisture content of the grain, in kg/kg; k_{eff} is the effective thermal conductivity of the grain pile, in W/(m·K); ρ_b is the grain pile density, in kg/m^3; T is the temperature, in K; and h_{fg} is the latent heat of evaporation of grain piles, in W/(m^2·K).

According to the law of conservation of mass, the governing equation for moisture transfer within the grain pile is the following:

$$\frac{\partial(\varepsilon_a \rho_a w)}{\partial t} + \nabla \cdot (\rho_a u w) = \nabla \cdot \left(\rho_a D_{eff} \nabla w\right) - (1-\varepsilon_a)\rho_b \frac{\partial W_w}{\partial t} \tag{3}$$

where ρ_a is the density of air, in kg/m^3; w is the absolute moisture content of the air between the grains, in kg/kg; u is the velocity of air, in m/s; and D_{eff} is the effective diffusion coefficient of moisture through the grain pile, in m^2/s.

The momentum transfer equation within the grain pile is the following:

$$\frac{\partial u}{\partial t} + (u \cdot \nabla)u = -\frac{\nabla p}{\rho_a} + \nabla \cdot \left(\frac{\mu}{\rho_a} \nabla u\right) - \frac{150\mu(1-\varepsilon_a)^2}{{\varepsilon_a}^3 {d_p}^2} u - \frac{1.75\rho_a(1-\varepsilon_a)}{{\varepsilon_a}^3 d_p} |u| u \tag{4}$$

where μ is the dynamic viscosity of the fluid, in Pa·s; p is the stresses, in Pa; and d_p is the equivalent diameter of grain particles, in mm.

The ventilation and heat transfer problems can be solved by these Equations [19–21] (Equations (1) to (4)); however, describing the concentration distribution and transport properties of ozone within the grain pile requires solving the ozone component transport equation. The ozone and air mixture flow within the grain pile is assumed to be a laminar flow of an ideal mixture of gases. Due to the different reaction rates of ozone in solid-

phase grain particles and gas-phase intergranular air, two separate component transport equations are required [17]:

$$\varepsilon_g \frac{\partial}{\partial t}(\rho_g w_g) + \nabla \cdot (\rho_g w_g) = \varepsilon_g \nabla \cdot (\rho_g D_g \nabla w_g) - k_1 \varepsilon_g \rho_g w_g - \rho_g h_m A_s (w_g - w_{ss}) \quad (5)$$

$$(1 - \varepsilon_g) \frac{\partial}{\partial t}(\rho_s w_s) = (1 - \varepsilon_g) \nabla \cdot (\rho_s D_s \nabla w_s) + \rho_g h_m A_s (w_g - w_{ss}) - k_2 (1 - \varepsilon_g) \rho_s w_s \quad (6)$$

where ε_g is the porosity of grain pile; w_s is the mass fraction of ozone in the grain; w_{ss} is the mass fraction of ozone on the surface of the grain particles; w_g is the mass fraction of air between grain particles; ρ_g is the density of the gas, in kg/m^3; ρ_s is the particle density of the grain pile, in kg/m^3; k_1 is the decomposition reaction constant of ozone in the air between the grains; k_2 is the reaction constant for the interaction between ozone and grain; h_m is the mass transfer coefficient, in m/s; D_g is the diffusion coefficient of ozone in the air, in m^2/s; and D_s is the diffusion coefficient of ozone in solids of porous media, in m^2/s. The transport equation has $\rho_g = \rho_a$, $\rho_s = \rho_b$.

2.3. Boundary Conditions and Related Parameters

The focus of this simulation study was a wheat pile characterized by a porosity of 0.4. The initial distribution of temperature and moisture within the grain pile was uniform. The grain pile area was treated as a porous medium, while the upper part of the pile constituted an air region. The temperature in the air region was consistent with the temperature of the grain pile and had an average value of 30 °C. Initially, the grain moisture content was 12.75%, and the incoming air had a relative humidity of 63%. A summary of the pertinent physical parameters of both the wheat and the air can be found in Table 1.

Table 1. Physical parameters related to wheat and air [22].

Parameters	Physical Parameter	Parameter Value
Wheat parameters	Densities ρ_w (kg/m^3)	762
	Thermal conductivity k_w (W/(m·K))	0.16
	Thermal capacity C_w (J/(kg·K))	1300
	Permeability K/m^2	7.27×10^{-9}
	Porosity ε	0.4
	Tortuosity τ_w	1.15
Air parameters	Densities ρ_a (kg/m^3)	1.225
	Thermal conductivity k_a (W/(m·K))	0.0242
	Thermal capacity C_a (J/(kg·K))	1006.43
	Dynamic viscosity μ (Pa·s)	1.79×10^{-5}

The ventilation system employed in this study followed a water retention ventilation approach, utilizing mass flow inlets and pressure outlets. The unit air volume for this grain pile was 5 m^3/(h·t), a common practice in storehouses. As the temperature of the grain pile exhibited minimal changes, the alterations in air density within the storehouse were considered negligible. Consequently, each inlet ventilation utilized a mass flow rate of 0.86 kg/s. The temperature of the incoming air was 22 °C, which was 8 °C lower than the temperature of the grain pile, and the moisture level was 63%. The initial ozone concentration at the inlet was 0.1 mg/L, with a mass flow rate of 1.03×10^{-3} kg/h. The amount of ozone fumigation in stored grain cannot exceed 0.2 mg/L, so the inlet ozone concentration is adjusted to 0.2 mg/L in the fumigation condition 3. Ozone fumigation was carried out continuously for 24 h per day, spanning a total duration of 12 days. Considering the space size and grain storage requirements, and according to industry norms, referring to common parameters, we selected the following three working conditions. The parameters of the three working conditions are shown in Table 2.

Table 2. The parameters of the three working conditions.

Condition	Ventilation Condition 1	Fumigation Condition 2	Fumigation Condition 3
Initial grain temperature	30 °C	30 °C	30 °C
Initial grain moisture	14.61%	14.61%	14.61%
Inlet air temperature	22 °C	\	\
Inlet air moisture	63%	\	\
Unit air volume	5 $m^3/(h{\cdot}t)$	\	\
Work time	7 d	15 d	15 d
Inlet ozone concentration	\	0.1 mg/L	0.2 mg/L

2.4. Grid-Independent Verification and Mathematical Model Validation

The resolution of all mathematical equations was accomplished through the utilization of the commercial software Fluent. The physical model of the storehouse was solved at 1,261,163, 1,769,007, 2,699,897, and 4,489,068 meshes numbers. The average grain temperature and moisture content during 24 h ventilation were compared to determine the optimal mesh number and quality [23]. The results of the calculations are shown in Figure 3.

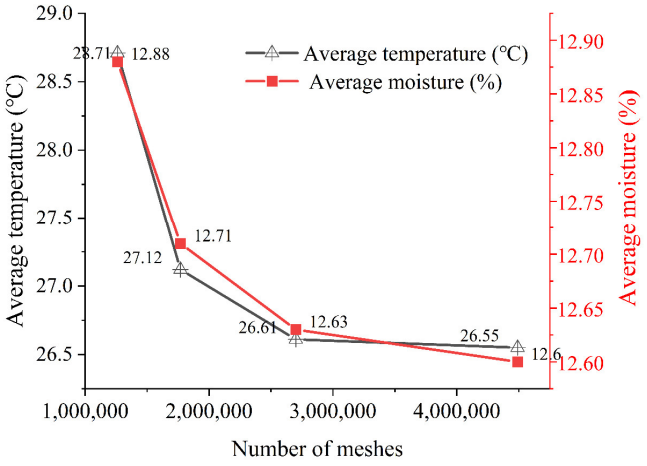

Figure 3. Comparison of calculation results for different numbers of meshes.

As shown in Figure 3, an increase in the number of meshes results in a gradual reduction in variations in the average temperature and moisture of the grain pile. Notably, starting from the number of meshes of 2,699,897, these variations became considerably smaller when compared to the previous mesh configurations. After a comprehensive assessment of both calculation accuracy and computational efficiency, the final selection for the number of meshes was determined to be 2,699,897.

To validate the accuracy of the ozone transport model, the simulation data were compared with experimental results. The experimental setup comprised a small cylindrical silo with a diameter of 0.1 m and a height of 1.2 m. The lower end of the silo was connected to an ozone generator and an oxygen concentrator, while the upper end was connected to a glass container designed for ozone disposal. Positioned at the top of the silo was a cage containing 50 spotted valley robber beetles and an appropriate quantity of grain, which was employed to assess the mortality rate of the pests. The mass concentration of ozone utilized in the experiment was 2.2 mg/L. The numerical simulation of the physical model involved a cylinder with a diameter of 0.1 m and a height of 1.0 m, and the user-defined function (UDF) method was used in the numerical calculation [17]. The numerical calculation of the ozone concentration at the top of the column was compared with the experimental results, as shown in Figure 4.

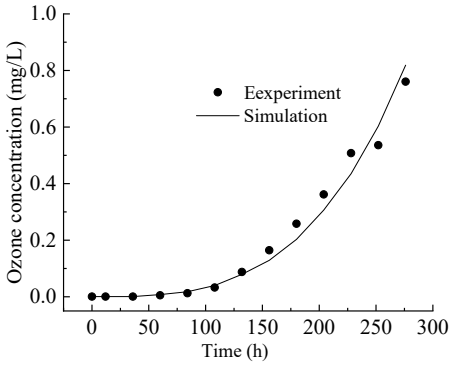

Figure 4. Comparison of experimental results [17] and simulated data.

It is evident from the results that the simulated data exhibit a higher degree of consistency with the experimentally measured data. In general, the trend in the measured ozone concentration aligns with the simulation results, thereby affirming the reliability of the simulation method for modeling the ozone diffusion process using the UDF.

3. Results and Discussion

3.1. Comparative Analysis of Temperature in Grain Pile

Figure 5 shows the temperature distribution within the grain pile at Y = 13.8 m. This specific Y = 13.8 m corresponds to the cross-section of the second primary duct spanning the grain pile. In the MVN, a vertical duct is positioned at this cross-section, making it an ideal choice for our simulation study. As shown in Figure 5, the temperature within the grain pile exhibits a pronounced stratification pattern along the vertical height. This phenomenon arises from the fact that the upward-moving air undergoes heat exchange with the relatively warmer grain pile. As the air ascends, its temperature gradually rises, and it becomes less effective at absorbing heat from the hotter grain pile. Consequently, this results in varying rates of temperature reduction at different positions within the grain pile as one moves away from the ventilation channel. Furthermore, the inherent thermal resistance of the wheat grains exacerbates the stratification of the temperature distribution within the grain pile.

The undulating temperature distribution observed in the MVN arises from the varying cooling rates at the location of the vertical ducts compared to the spaces between them. Vertical ducts have significantly reduced the resistance to airflow in the vertical direction, resulting in a notable increase in the propulsion velocity of the inlet in that same direction. Grain piles situated directly above the vertical ducts experience accelerated cooling, causing the cold front to progress more swiftly compared to grain piles without nearby vertical ducts. This contrast manifests as convex shapes on the temperature cloud map, whereas the areas between two risers exhibit concave valley shapes. In contrast, in the OVN, this cross-section of the grain pile is predominantly influenced by the main ducts at ground level. Here, the airflow is evenly distributed, and the cold fronts advance along a horizontal plane, resulting in a more uniform temperature distribution across the grain pile.

Figure 5c,d demonstrates that on the second day of ventilation, the leading edge of the cold front in the MVN has advanced well beyond the grain pile, engaging in heat exchange with the air above the pile. In contrast, the cold front in the OVN has just reached the surface of the grain. As shown in Figure 5e, following 3 days of ventilation, the average temperature of the grain pile under the MVN stabilizes at approximately 22.31 °C. This proves the superior cooling efficiency of the MVN, meeting the requirements for safe grain storage.

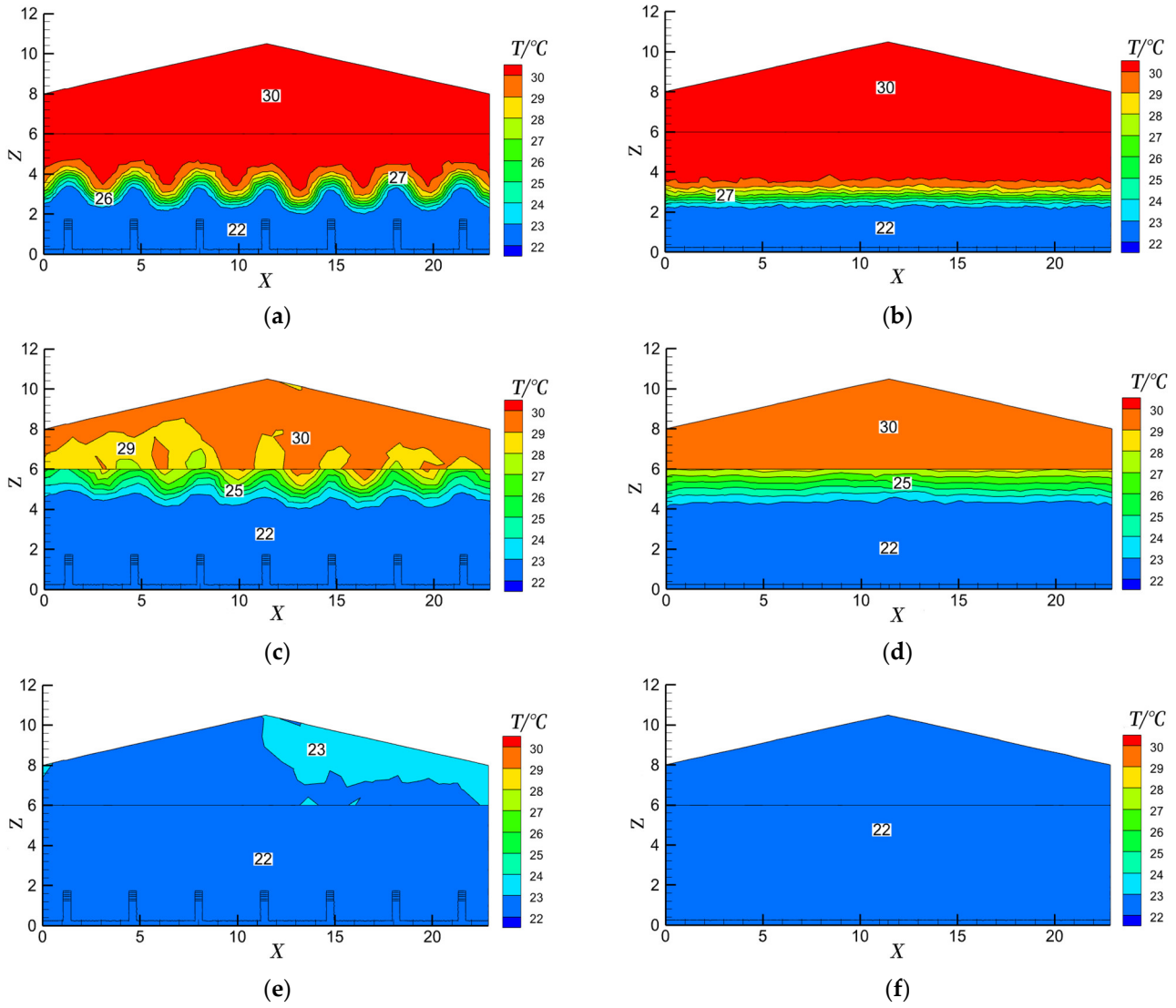

Figure 5. Distribution of temperature at different times. (**a**) First day (MVN); (**b**) first day (OVN); (**c**) second day (MVN); (**d**) second day (OVN); (**e**) third day (MVN); (**f**) third day (OVN).

In summary, the MVN has successfully achieved the objective of shortening the air's path within the grain pile, consequently enhancing the speed of cold front advancement in the vertical direction of the grain pile.

Figure 6 shows the temperature curve of the grain pile, as well as a comparison of different grain layers, over 7 days of ventilation under the two ventilation networks. Notably, the MVN exhibits superior cooling effectiveness compared to the OVN on the second day. The most substantial average temperature discrepancy occurs on the initial day of ventilation, amounting to approximately 0.48 °C. There is little divergence in cooling efficiency between the two ventilation networks following the second day of ventilation.

In Figure 6b, it is evident that the maximum temperature of the grain pile undergoes minimal variation in the two days before ventilation commencement. This phenomenon arises from the time required for the incoming air to permeate the grain pile. At the outset of the ventilation period, the upper segment of the grain pile fails to engage in heat exchange with the incoming air, resulting in the pile's temperature remaining at an initial value of around 30 °C. This discrepancy is attributable to the vertical ducts of the MVN, which partition a part of the air volume. As ventilation duration increases, the maximum temperature of the MVN experiences a more rapid decline compared to the OVN.

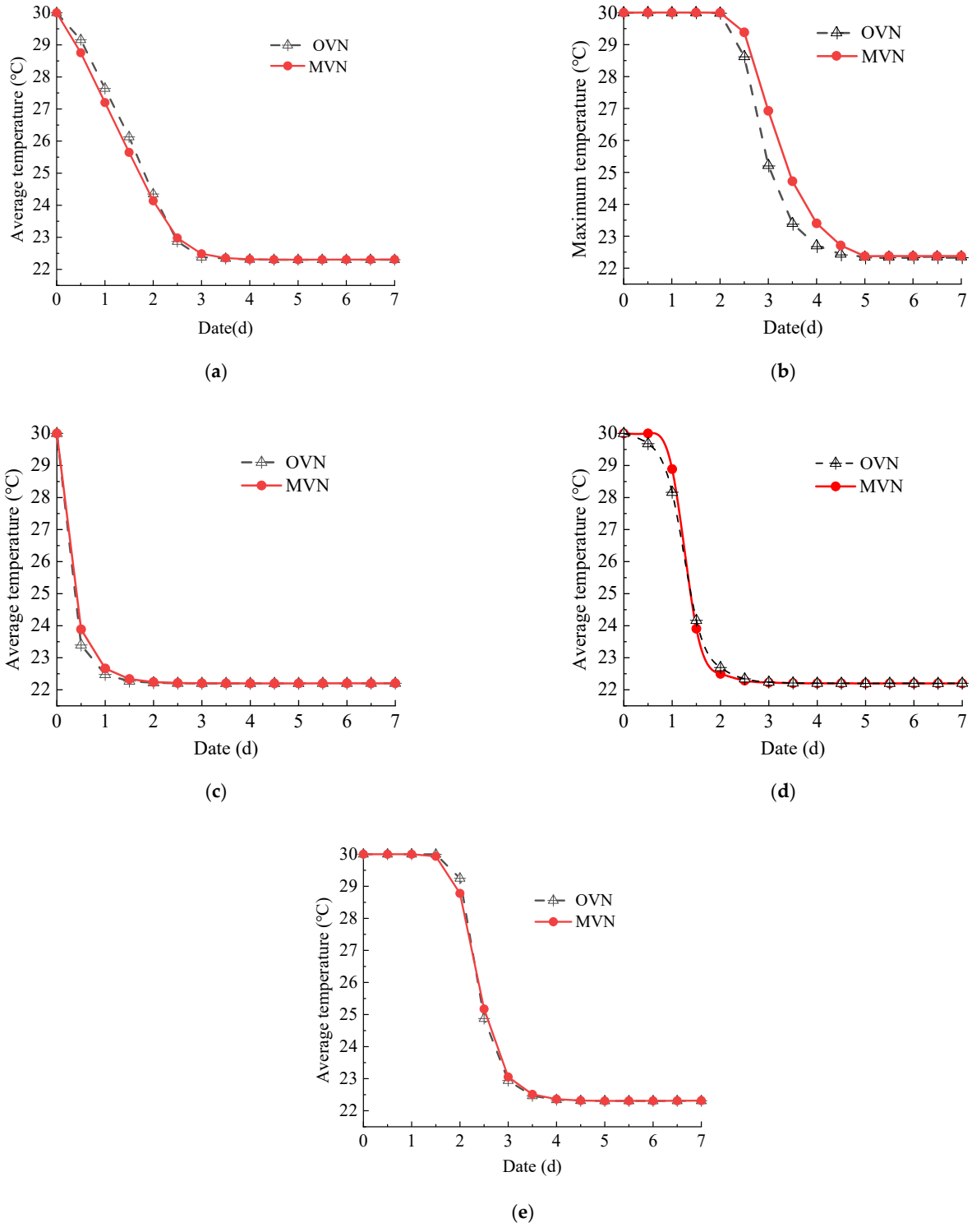

Figure 6. Comparison of temperature at different grain layers. (**a**) Average temperature; (**b**) maximum temperature; (**c**) 0.5 m grain layer; (**d**) 3.0 m grain layer; (**e**) 5.5 m grain layer.

Figure 6c–e shows three-line graphs detailing temperature comparisons for grain layers situated at 0.5 m, 3.0 m, and 5.5 m heights, respectively. The 0.5 m grain layer predominantly encompasses ventilation ducts on the ground level, resulting in a superior cooling effect for the OVN. The cooling rate of the OVN is 0.51 °C/d and the cooling rate of the MVN is 0.55 °C/d. In the 3.0 m and 5.5 m grain layers, the temperature of the grain pile remained relatively constant under both ventilation networks after the fifth day of

ventilation. The final temperature of the grain pile settled at around 22.30 °C. However, it is noteworthy that the temperature of the grain pile under the MVN exhibited an earlier and more rapid change. This observation underscores the enhanced cooling efficiency of the MVN, which is capable of swiftly bringing down the grain temperature to a safe range in a short period. Optimized ventilation systems can provide faster air flow, helping to distribute temperature and humidity more evenly in the grain pile, thus slowing potential hot spot formation. It can prevent the growth of mold and fungi, reducing mildew and quality loss. Slowing down the oxidation reaction in grains helps to maintain the nutritional value and storage stability of grains. In addition, the MVN can be retrofitted directly onto an existing OVN at a lower cost than an all-new design.

3.2. Comparative Analysis of the Grain Moisture Content in Grain Pile

Figure 7 shows the comparison between the two ventilation networks within the Y = 13.8 m cross-section, specifically regarding the moisture content of the grain pile. The average moisture content along the vertical direction of the grain pile exhibits an initial decline followed by a minor subsequent increase for ventilation in both networks. The primary reason behind the decrease in the average moisture content of the grain pile is the disparity in the partial pressure of water vapor between the incoming air and that within the grain pile. This discrepancy prompts a moisture gradient, causing moisture within the grain pile to diffuse into the air, thereby reducing the overall moisture content of the pile.

As the ventilation process continues, the partial pressure of water vapor on the surface of the grain pile gradually diminishes. Consequently, when the partial pressure of water vapor in the incoming air surpasses that on the surface of the grain, the direction of moisture migration reverses, shifting from the air back into the grain pile. This reversal leads to a slight increase in the moisture content of the pile. Overall, the fluctuation in moisture content observed in the grain pile during ventilation reflects the dynamic interplay between the moisture levels in the incoming air and those within the grain pile, dictated by the shifting partial pressures and moisture gradients.

In Figure 7g, we observe that during the initial 2.5 days of ventilation, the average moisture content of the grain pile consistently decreased. This decreasing trend in moisture content was consistent for both ventilation networks, with both reaching approximately 12.63%. However, as the ventilation process continued, there was a slight rebound in the average moisture content of the grain pile. By the seventh day of ventilation, the average moisture content for both ventilation networks had stabilized at 12.64%, representing a 0.8% drop compared to the initial levels. As shown in Figure 7a–f, on the first day of ventilation, the highest moisture levels in the grain pile were concentrated in the lower section of the pile on both sides of the ventilation channel, near the vent position. As the ventilation process progressed, the area with elevated moisture levels within the pile gradually expanded.

By the third day of ventilation, the highest moisture content had reached 12.78%, surpassing the initial stack moisture of 12.75%. This can be attributed to the low temperature of the incoming air. In this area, the grain pile remains in contact with the cold airflow from the incoming air, causing a rapid reduction in the temperature of the grain pile. Consequently, moisture in the higher-temperature regions of the grain pile migrates toward the cooler areas, leading to an accumulation of water vapor in the lower-temperature regions. Furthermore, due to the significant hygroscopic nature of the grain particles, the moisture content of the grain pile near the ventilation channel increases. Therefore, when employing mechanical ventilation in grain silos, it is crucial to reasonably control the duration of ventilation and avoid excessively prolonged ventilation, as continuous moisture absorption by the grain pile may lead to mold growth.

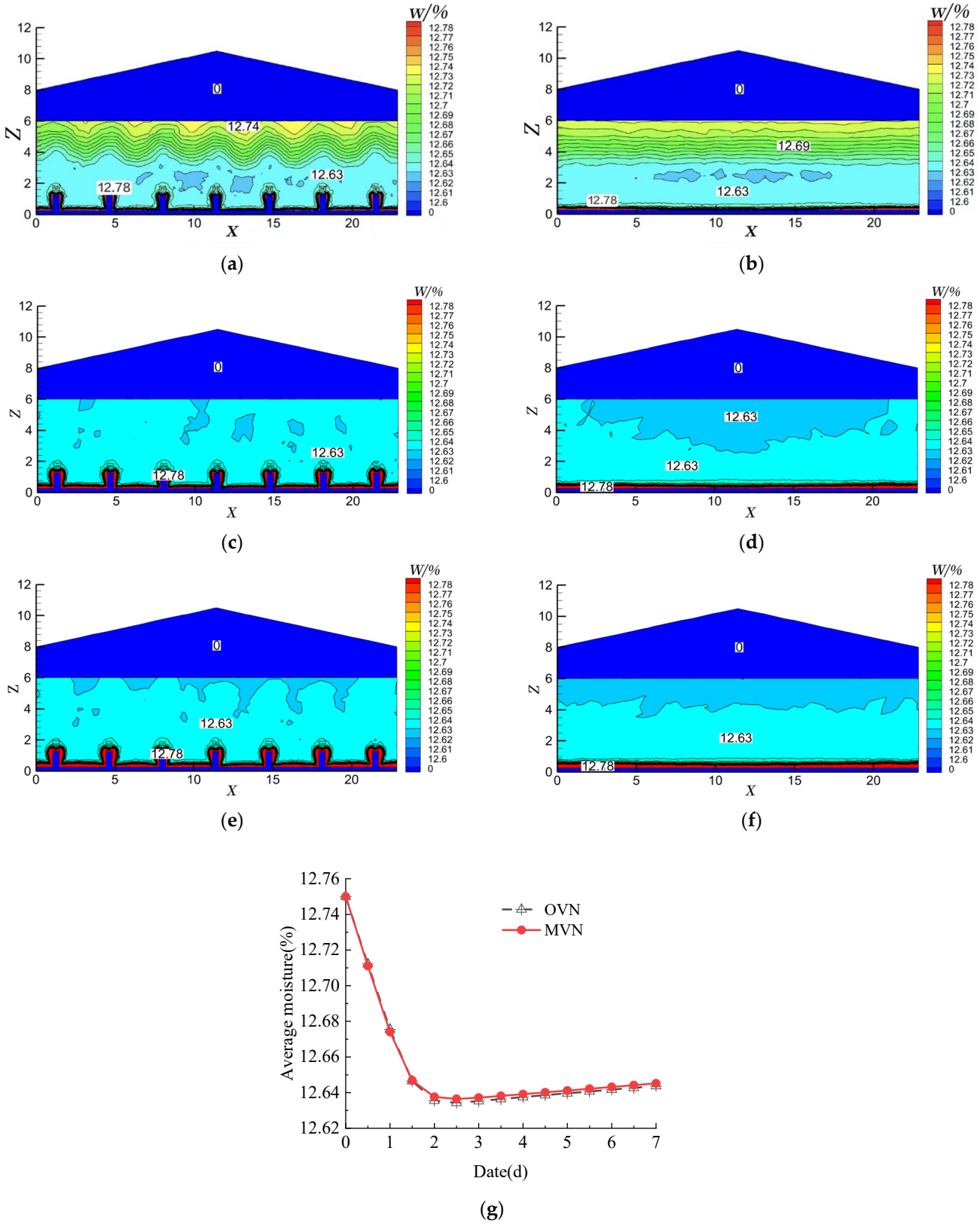

Figure 7. Distribution of moisture content at different times. (**a**) First day (MVN); (**b**) first day (OVN); (**c**) second day (MVN); (**d**) second day (OVN); (**e**) third day (MVN); (**f**) third day (OVN); (**g**) average moisture.

Figure 8 presents a line graph comparing the average moisture levels in grain layers at various heights within the two ventilation networks. Despite differences in the height of the grain layers, the general trend in moisture change is consistent between the two ventilation networks. Within the 0.5 m grain layer, after one day of desorption, the pile entered a phase of continuous moisture absorption, with the MVN exhibiting stronger moisture absorption capabilities. In the 3.0 m grain layer, the moisture decline pattern for both ventilation networks was largely identical. After two days of ventilation, the average moisture content of the grain pile reduced to 12.63%, and the range of grain moisture decreased by 0.9% compared to the initial moisture level. Subsequent ventilation had minimal impact on the moisture content of the grain pile. In the 5.5 m grain layer, the moisture decline curve for the first two days of ventilation under both ventilation networks was closely mirrored. The MVN demonstrated enhanced moisture retention capabilities.

In summary, the MVN effectively manages grain moisture, keeping it within a safe range, thus preventing mold growth and deterioration. This ensures the safety and quality of stored grain.

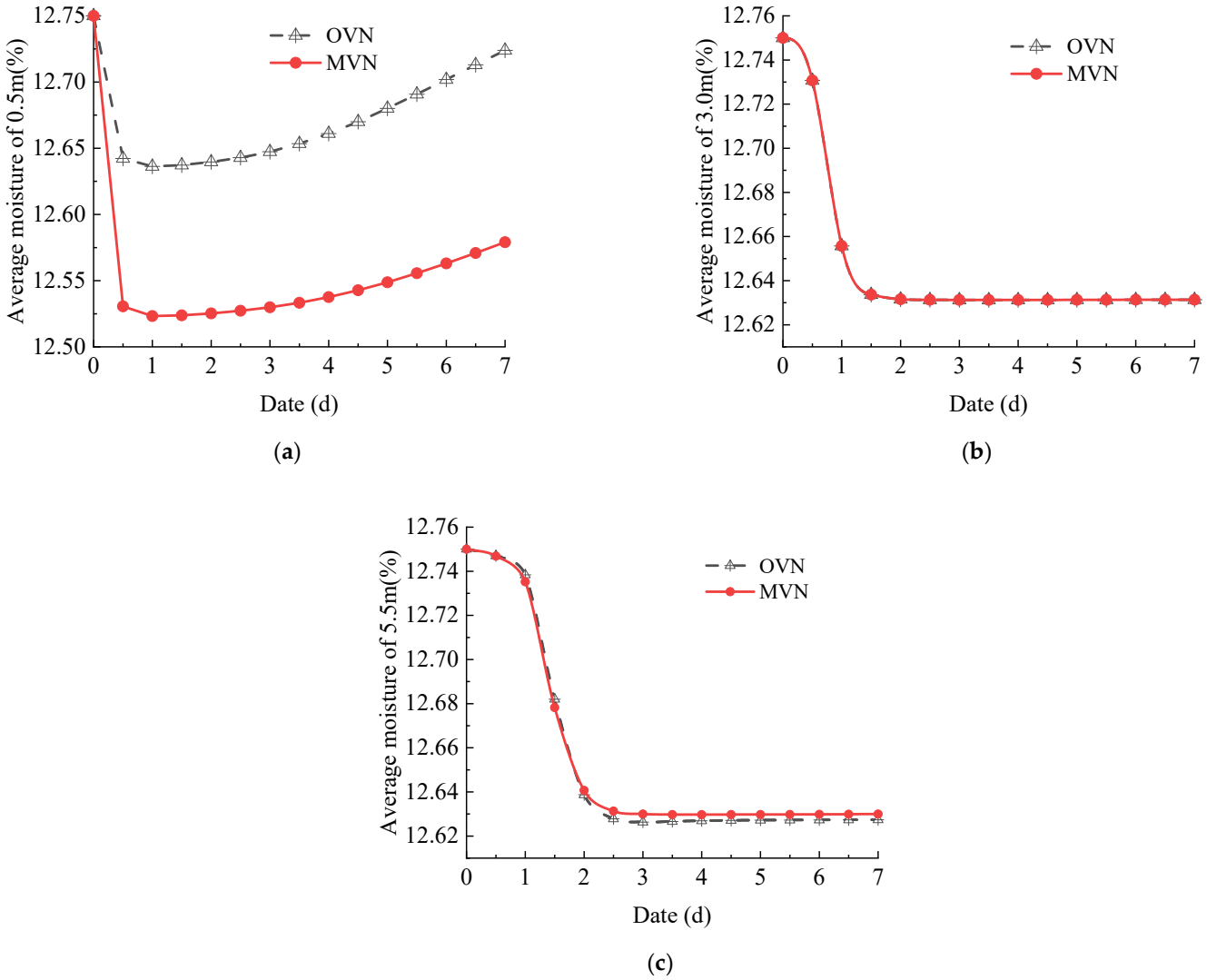

Figure 8. Comparison of average moisture content in different grain layers. (**a**) The 0.5 m grain layer; (**b**) 3.0 m grain layer; (**c**) 5.5 m grain layer.

3.3. Analysis of Ozone Migration Characteristics in Grain Pile

3.3.1. Analysis of the Migration Pattern of Ozone Concentration with Time in Grain Pile

Figure 9 provides a visual representation of ozone concentration distribution during various fumigation durations at Y = 13.8 m within the two ventilation networks. Y = 13.8 m is a pivotal location along the length, featuring vertical ducts, making it a representative point for analysis. The analysis of the ozone concentration distribution in the grain pile under the MVN reveals a distinctive wave-like pattern in the lateral direction. Notably, high ozone concentrations progress more rapidly near the risers positioned adjacent to the ventilation channel's openings. This phenomenon can be attributed to the faster ozone flow rate near the inlet. Conversely, in the OVN, the high concentrations encounter greater resistance when ascending.

On the second day of fumigation, a comparison between Figures 9a and 9b shows that ozone in the MVN penetrates as far as the 8.8 m grain layer, whereas in the original network, ozone only reaches up to 3.6 m. This disparity arises from the introduction of vertical ducts in the MVN, and the higher ozone flow rate compared to the OVN. The inclusion of vertical ducts in the MVN accelerates the movement of high-concentration ozone, resulting in less attenuation. This effect becomes more pronounced with increasing grain pile height. However, the region between the two risers in the MVN experiences lower ozone concentration due to the influence of the risers, in contrast to the equivalent area in the OVN. On the seventh day of fumigation, a comparison of Figure 9c,d reveals that ozone has permeated the grain surface in the MVN. IN comparison, as for the OVN, ozone just appeared on the surface of the particles.

Referring to Figure 9g, it is evident that during the initial 10 days of fumigation, both ventilation networks exhibited a notably faster diffusion rate of average ozone concentration. Over the following days, the variation in ozone concentration over time became minimal after the 12th day, with both networks reaching a concentration of 0.078 mg/L by the 15th day of fumigation. In the first 7 days, the average ozone concentration in the MVN surpassed that of the OVN.

However, from the 7th to the 15th day, the MVN registered lower ozone concentrations, underscoring the more pronounced advantage of the MVN during the pre-fumigation period. According to existing literature sources [24], common pests like corn weevils, grain borers, longhorn grain borers, red grain borers, and rusty red grain borers exhibited mortality after exposure to ozone concentrations of 10 mL/m^3 (equivalent to 0.0218 mg/L) for varying durations: 5.5, 12, 13, 18, and 13.5 days, respectively. Higher ozone concentrations led to shorter pest survival times. Therefore, it can be inferred that the ozone concentration within the grain pile on the 15th day was already significantly effective in inhibiting pest activities.

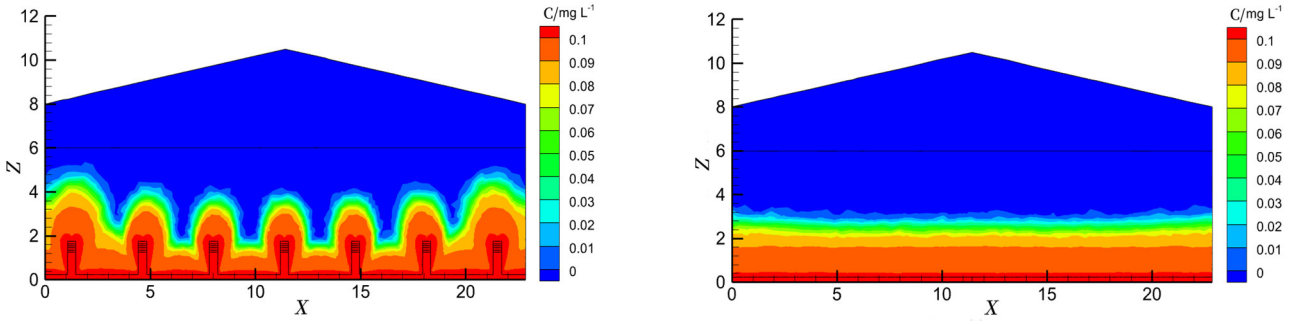

(**a**) (**b**)

Figure 9. *Cont.*

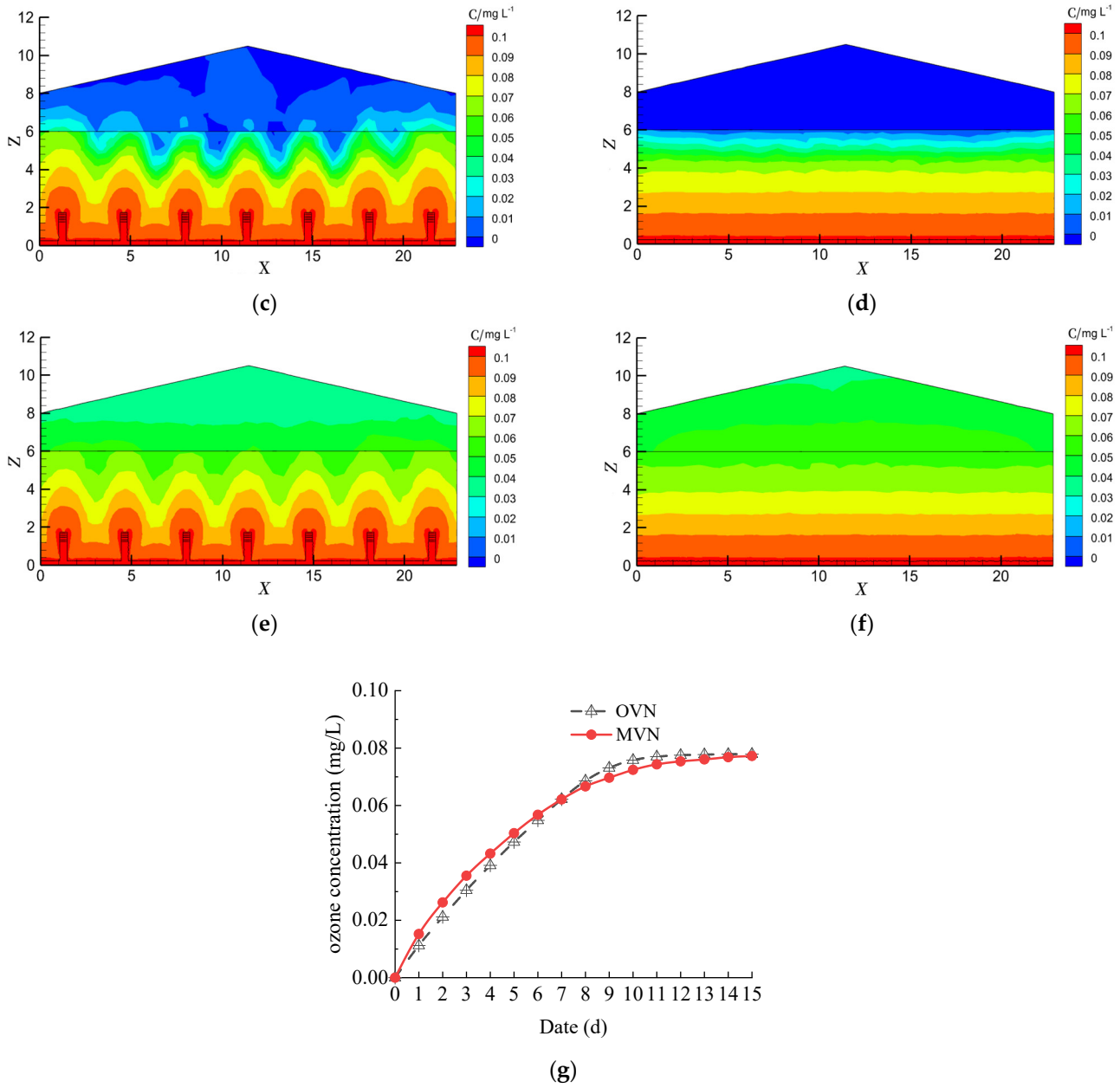

Figure 9. Distribution of ozone concentration at different times. (**a**) Second day (MVN); (**b**) second day (OVN); (**c**) seventh day (MVN); (**d**) seventh day (OVN); (**e**) twelfth day (MVN); (**f**) twelfth day (OVN); (**g**) average ozone concentration.

3.3.2. Analysis of the Adsorbing Pattern of Ozone Concentration with Time in Grain Pile

During the fumigation process, grain pile particles tend to adsorb a portion of ozone molecules. Ozone has a strong oxidizing ability; when the concentration of ozone adsorbed by particles reaches a certain level, it will greatly reduce the quality of grain [25]. Therefore, it is crucial to investigate the concentration of adsorbed ozone on grain pile particles to ensure the safety of grain consumption.

Figure 10a,b shows the distribution of adsorbed ozone concentration within the grain pile at the Y = 13.8 m cross-section following 12 days of ozone fumigation. Notably, the distribution of ozone concentration adsorbed by the grain pile particles mirrors the distribution of ozone concentration within the grain pile. A distinct stratification pattern emerges, characterized by a higher concentration at the bottom, uniform dispersion within the OVN, and a ripple-like distribution in the MVN. This can be attributed to the increased

accessibility of ozone molecules to the grain pile particles in regions with elevated ozone concentrations, resulting in a higher concentration of adsorbed ozone.

Figure 10c shows the average concentration of adsorbed ozone in grain pile particles for the fumigation process. It is evident that during the initial 7 days, the average adsorbed ozone concentration in the grain pile under the MVN was nearly identical to that under the OVN. However, after the 7th day, the adsorbed ozone concentration in grain pile particles under the MVN surpassed that of the OVN. This shift can be attributed to the introduction of vertical ducts, which increased the contact surface area between the ventilation channels and the grain pile. As a result, the total amount of ozone adsorbed by the grain pile became greater.

After the 12th day, the rate of change in adsorbed ozone concentration became notably small. Additionally, the maximum concentration of ozone molecules adsorbed by the grain particles registered at only 1.6×10^{-8} mg/L, which had little effect on grain quality [26,27]. Furthermore, due to the labile decomposition of ozone, this concentration tends to diminish even further over time.

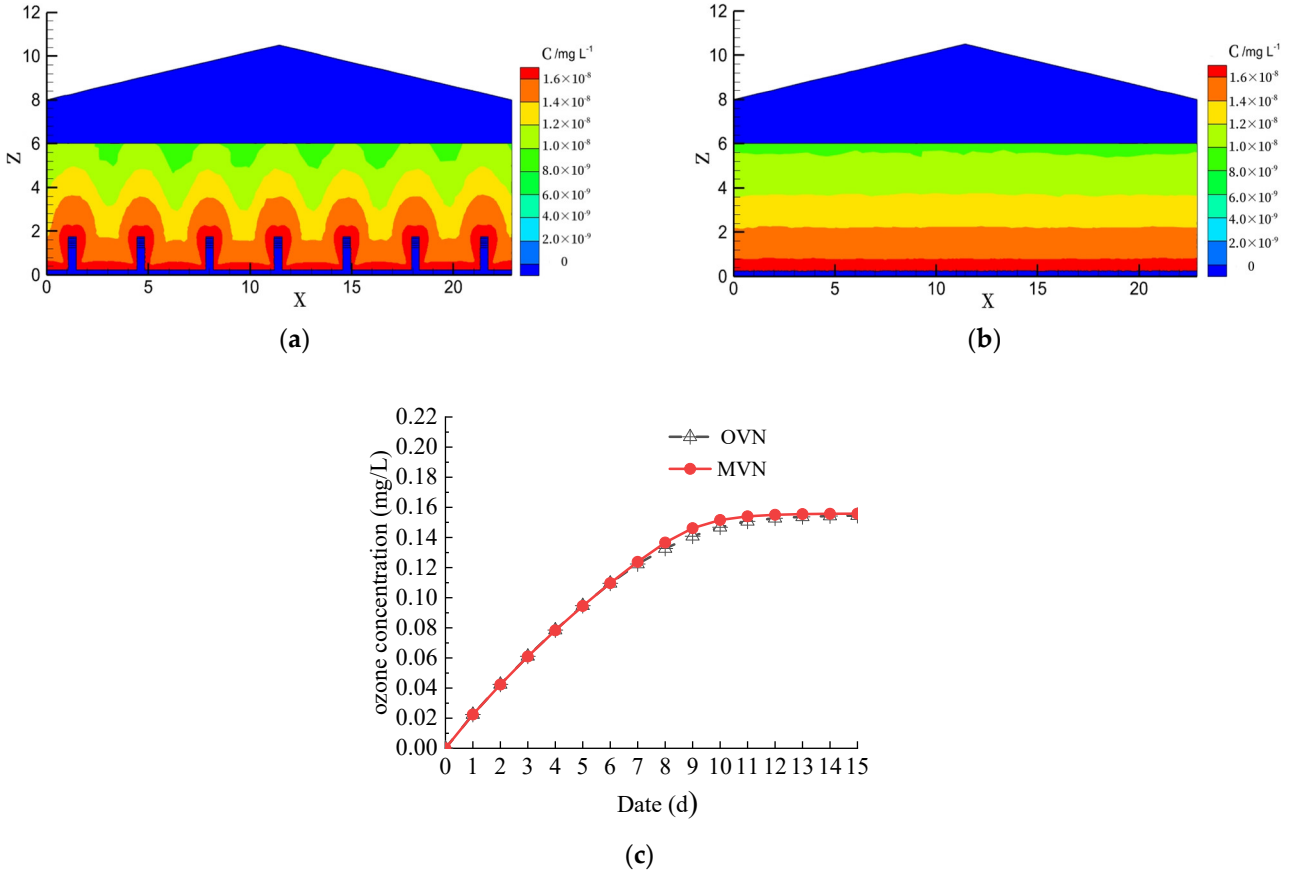

Figure 10. Ozone concentration adsorbed by grain pile particles. (**a**) Y = 13.8 m (MVN); (**b**) Y = 13.8 m (OVN); (**c**) average adsorbed ozone concentration on grain pile particles.

3.3.3. Analysis of Ozone Transport Patterns at Different Heights and Lengths of Grain Pile

Figure 11 shows the distribution of ozone concentrations across various height and length profiles within the grain pile on the seventh day of ozone fumigation. At the 0.5 m grain layer, the average ozone concentration was notably higher due to the proximity to the ventilation ducts. Conversely, lower ozone concentrations were observed in the area between the two branch ducts and on both sides near the wall position.

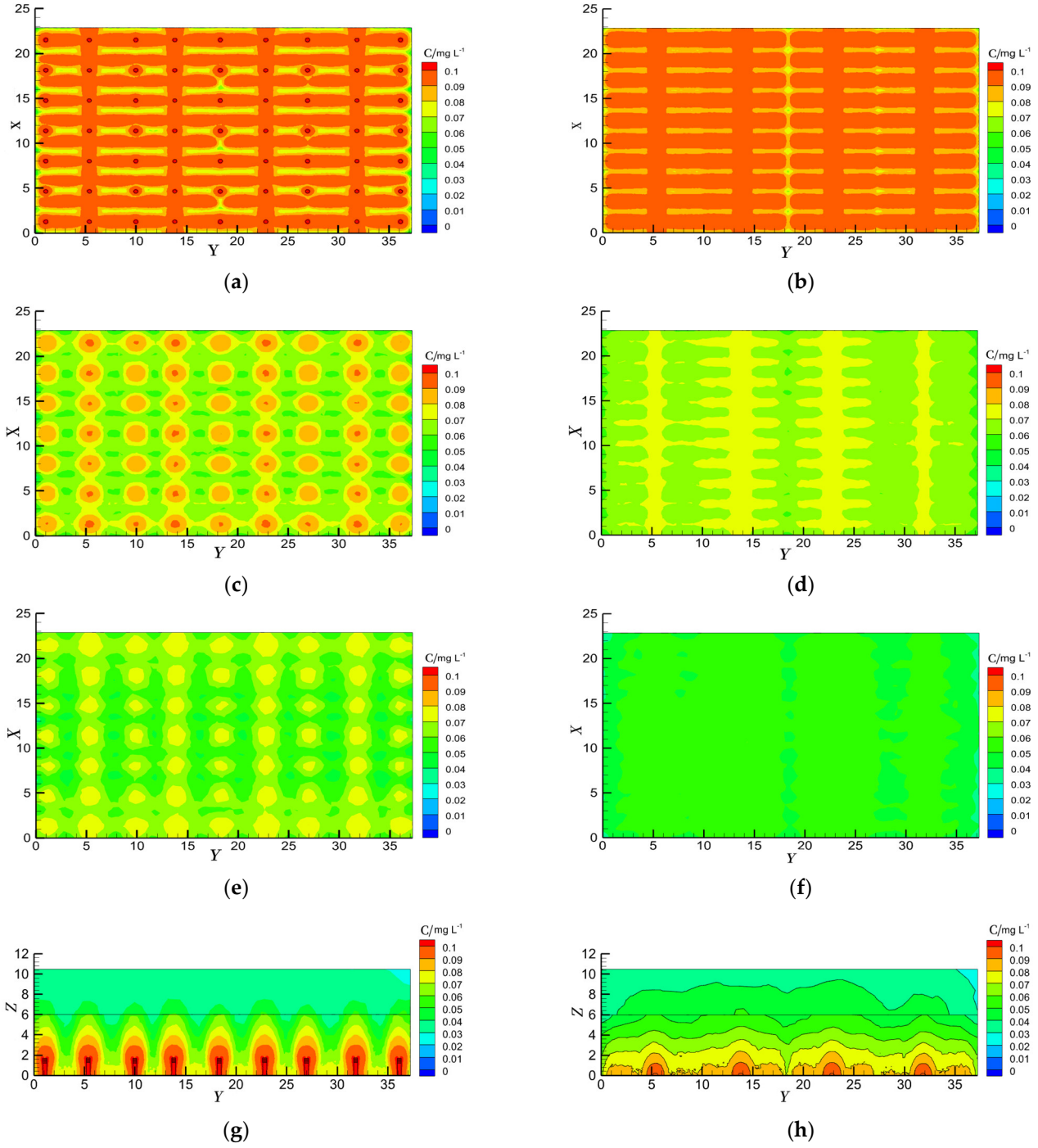

Figure 11. Distribution of ozone concentration at different height and length on the seventh day. (**a**) Z = 0.5 m (MVN); (**b**) Z = 0.5 m (OVN); (**c**) Z = 3.0 m (MVN); (**d**) Z = 3.0 m (OVN); (**e**) Z = 5.5 m (MVN); (**f**) Z = 5.5 m (OVN); (**g**) X = 11.83 m (MVN); (**h**) X = 11.83 m (OVN).

Moving to the 3.0 m grain layer, the high ozone concentration present at the vertical ducts' position in the MVN extended to this level. In contrast, the OVN exhibited relatively lower concentrations in other areas. At the 5.5 m grain layer, the average ozone concentration for the OVN was 0.06 mg/L. Comparatively, the ozone concentration in the vertical ducts of the MVN was slightly higher, at approximately 0.07 mg/L, while the concentration in other areas remained around 0.06 mg/L. This highlights that the inclusion of vertical ducts in the MVN enhanced the ozone propulsion speed and diminished flow resistance in the ventilation direction.

Figure 11g,h presents cloud diagrams on the YOZ cross-section, indicating that the ozone diffusion rate in the vertical duct is much faster than that at the same position in the OVN. The improved ventilation network redistributes a portion of the ozone through the addition of vertical risers, resulting in a significant fumigation advantage.

Figure 12 shows a line graph comparing ozone concentrations at various heights within the grain layer. The data reveal several noteworthy trends. In the 0.5 m grain layer, the ozone concentration of the OVN slightly exceeded that of the MVN. Moving to the 3.0 m grain layer, the average ozone concentration in the MVN exceeded that of the traditional OVN for the first six days of fumigation. Considering the 5.5 m grain layer, the MVN exhibited a high ozone concentration on the fifth day of fumigation, whereas the OVN reached a high ozone concentration on the seventh day of fumigation. Overall, the average ozone concentration in the MVN remained higher than that in the OVN for the initial nine days.

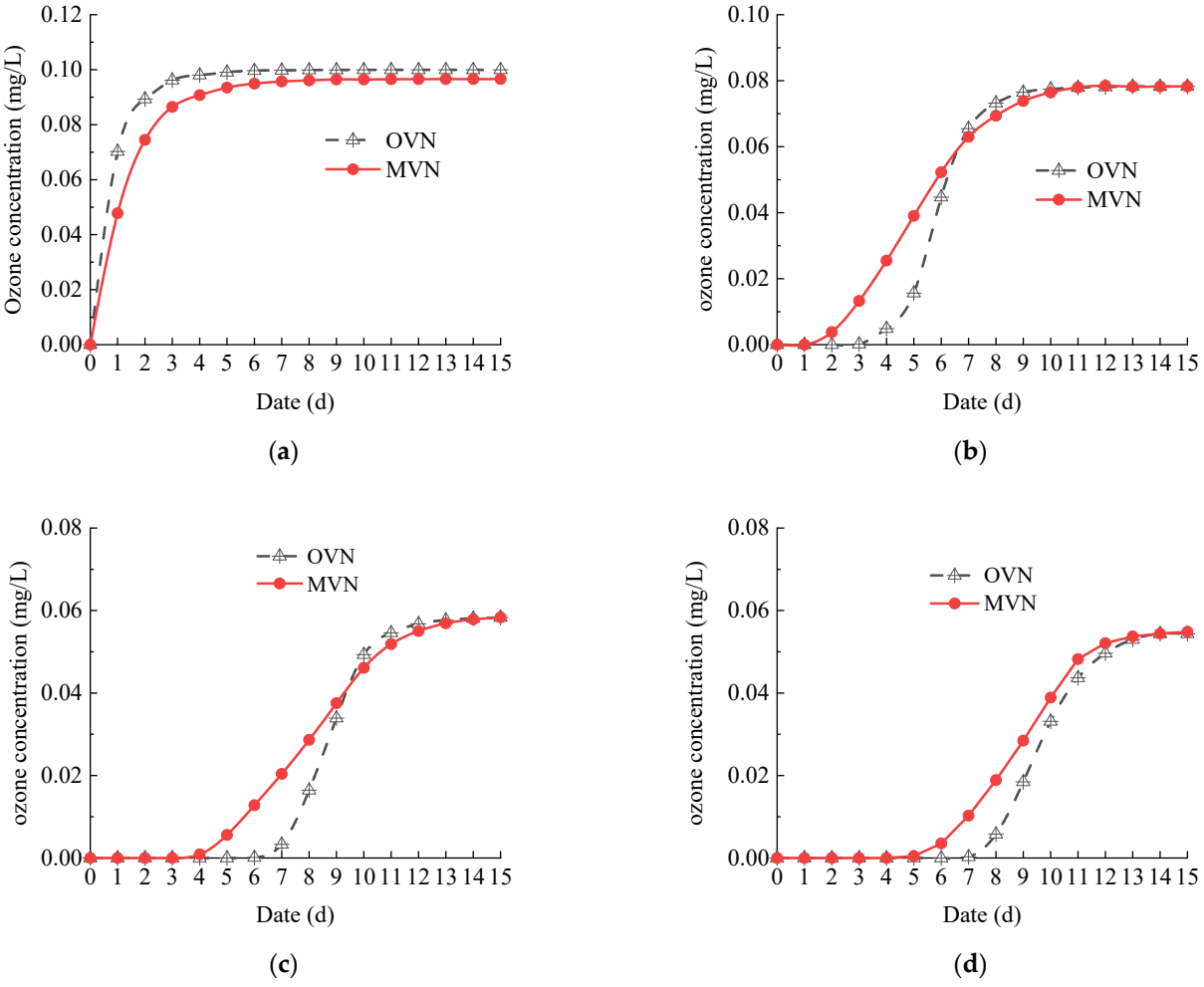

Figure 12. Comparison of ozone concentration at different grain layers. (**a**) The 0.5 m grain layer; (**b**) 3.0 m grain layer; (**c**) 5.5 m grain layer; (**d**) 6.0 m grain layer.

At the 6.0 m grain layer, the ozone concentration in both ventilation networks ultimately stabilized at 0.05 mg/L. Throughout the fumigation process, the average ozone concentration in the MVN was notably higher than that in the OVN. These analyses suggest that the MVN facilitated a faster ozone diffusion rate during the same fumigation period, proving more effective in eliminating pests concentrated in the upper area. As the height of the grain layer increased, the disparity in average ozone concentrations between the

two ventilation networks became increasingly pronounced, underscoring the growing advantage of the MVN.

3.3.4. Analysis of Transport Patterns at Different Inlet Ozone Concentrations

The above analysis delves into the distribution and migration patterns of ozone concentration within the grain pile under an ozone import volume of 0.1 mg/L. It was observed that, in the initial stages of fumigation, ozone concentrations were notably elevated in proximity to the ventilation ducts. As the fumigation process advanced, ozone gradually permeated the higher layers of the grain.

However, by the 15th day of fumigation, the average ozone concentration within the grain pile for both ventilation networks averaged around 0.078 mg/L. In specific areas of the upper grain layer, the average concentration dropped slightly to 0.058 mg/L, which remained relatively low. Consequently, adjustments were made to the ozone concentration at the inlet, raising it to 0.2 mg/L. This modification allowed for a subsequent evaluation of ozone concentration distribution within the grain pile. The outcomes of this study are depicted in Figure 13, with the 0.1 mg/L ozone concentration contour serving as the reference line.

In terms of the air between the grains, the average ozone concentration reached 0.1 mg/L on the fifth and sixth days for the MVN and the OVN, respectively. Upon comparing Figures 9g and 13e, both representing an imported ozone concentration of 0.1 mg/L, it was discerned that this adjustment did not significantly alter the trajectory of average ozone concentration within the grain pile over time. Notably, both networks exhibited higher concentrations than the MVN in the initial seven days.

Ozone concentrations quickly reached 0.1 mg/L at the 0.5 m grain layer due to the low ozone attenuation rate in this area close to the ventilation channel. The ozone concentration in the OVN was still higher than that in the MVN. At 3.0, 5.5, and 6.0 m, it took 6, 10, and 11 days for the MVN and 7, 10, and 12 days for the OVN to reach 0.1 mg/L. The advantages of the MVN were obvious in the pre-fumigation period and became more obvious with the increase in the height of the grain layer. Comparing Figure 13a–d with Figure 12a–d, it was found that the general trend of ozone concentration changes at different heights of grain pile at the imported 0.2 mg/L ozone concentration was generally the same as that at the imported 0.1 mg/L ozone concentration.

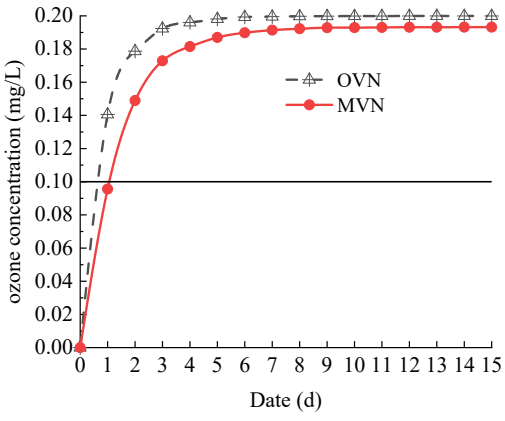

(**a**)

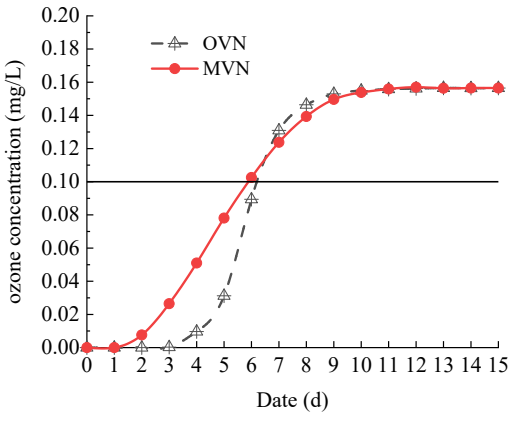

(**b**)

Figure 13. *Cont.*

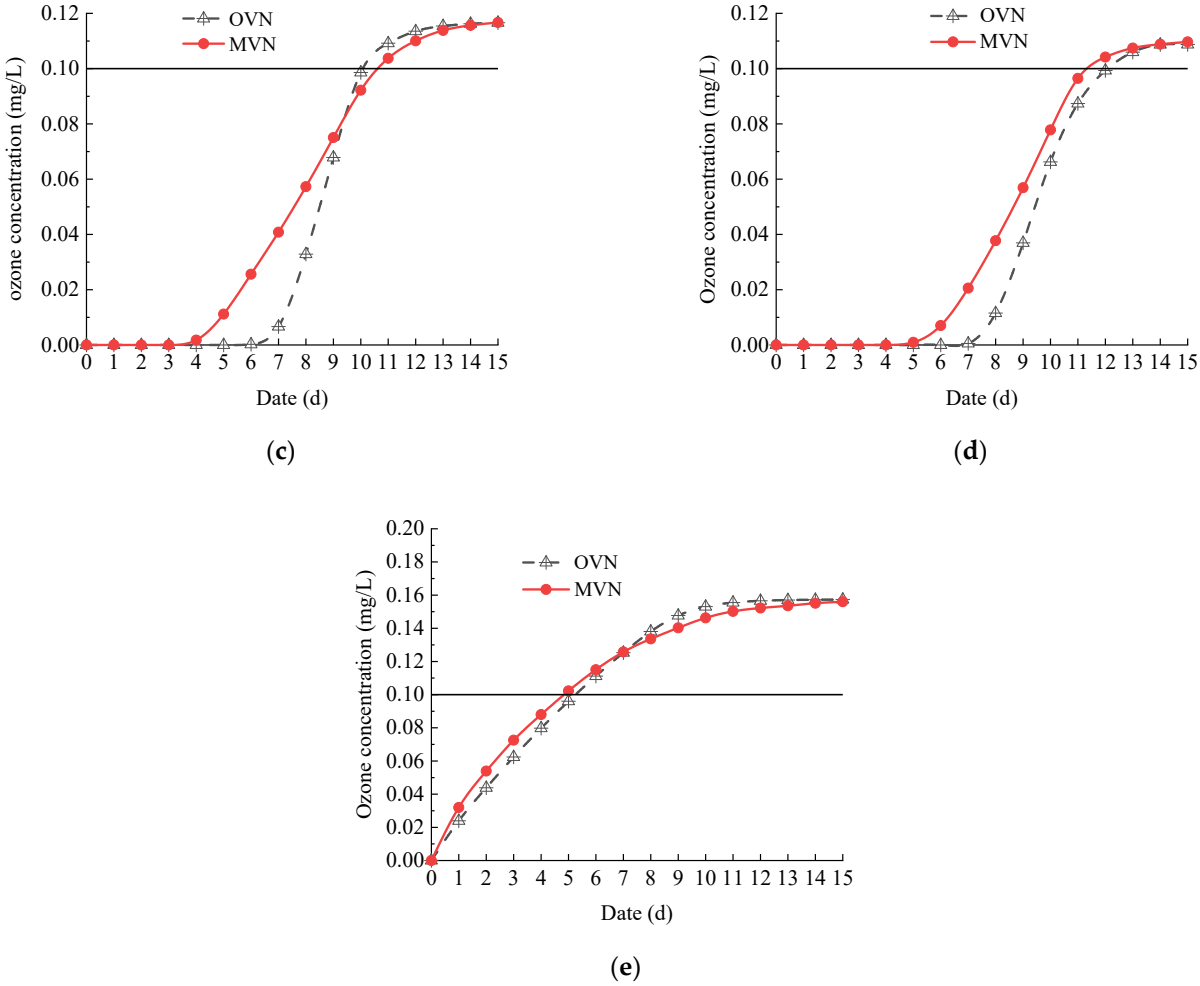

Figure 13. Comparison of ozone concentration at different grain layers at 0.2 mg/L inlet. (**a**) The 0.5 m grain layer; (**b**) 3.0 m grain layer; (**c**) 5.5 m grain layer; (**d**) 6.0 m grain layer; (**e**) average ozone concentration.

4. Conclusions

In this article, the ventilation effects and ozone migration within a grain pile were examined by conducting numerical simulations under the two different ventilation network configurations: the MVN and the OVN. The main conclusions that can be drawn are as follows:

First, the temperature, moisture content, and ozone concentration in the grain pile of the two ventilation networks are not evenly distributed in the vertical direction, showing a layered pattern. The horizontal direction of the MVN is wavy, while that of the OVN is approximately linear. Different height layers within the grain pile demonstrated varying trends in temperature and moisture changes. In addition, the MVN effectively lowers temperature and humidity levels compared to the OVN. The maximum average temperature difference appeared on the 1.5th day of ventilation, at about 0.48 °C. The vertical ducts added to the MVN improve the ventilation effect, ensuring the grain pile remains within safe parameters. It significantly improves the safety and quality of grain storage.

Finally, the advantage of the MVN is obvious in the early fumigation stage and high grain layers. On sixth day of fumigation, the average ozone concentration exceeded that of the OVN. The vertical ducts added to the MVN increase the speed of ozone advancing to the higher layer of the grain pile, providing enhanced control over pests and molds. The initial ozone concentration at the inlet had a limited impact on the average ozone concentration in the grain piles.

The ventilation effects and ozone concentration migration patterns in a grain pile under different ventilation networks are studied in this paper, and comprehensive analysis is carried out from many perspectives; however, due to the limitations in the author's ability and time, there are still many shortcomings in the research: the limitation of this study is that it does not consider the influence of variable porosity on the heat and moisture transfer process of the grain pile, which needs further exploration.

Author Contributions: Conceptualization, K.Y. and Y.W.; methodology, Y.M.; software, F.C. and X.D.; validation, K.Y. and F.C.; formal analysis, F.C.; investigation, Y.M. and X.D.; writing—original draft preparation, J.L. (Jiabin Li); writing—review and editing, J.L. (Jiying Liu); visualization, Y.M.; supervision, Y.W.; project administration, K.Y.; funding acquisition, K.Y. All authors have read and agreed to the published version of the manuscript.

Funding: The authors would like to thank the Scientific and Technological Project of Suzhou City and the Plan of Introduction and Cultivation for Young Innovative Talents in Colleges and Universities of Shandong Province.

Data Availability Statement: The data presented in this study are available on request from the corresponding author.

Conflicts of Interest: The authors declare that they have no known competing financial interests or personal relationships that could have appeared to influence the work reported in this paper. The authors declare that this work is not submitted to another journal.

References

1. Stathas, I.G.; Sakellaridis, A.C.; Papadelli, M.; Kapolos, J.; Papadimitriou, K.; Stathas, G.J. The Effects of Insect Infestation on Stored Agricultural Products and the Quality of Food. *Foods* **2023**, *12*, 2046. [CrossRef]
2. Mc Carthy, U.; Uysal, I.; Badia-Melis, R.; Mercier, S.; O'Donnell, C.; Ktenioudaki, A. Global Food Security—Issues, Challenges and Technological Solutions. *Trends Food Sci. Technol.* **2018**, *77*, 11–20. [CrossRef]
3. Taddese, M.; Dibaba, K.; Bayissa, W.; Hunde, D.; Mendesil, E.; Kassie, M.; Mutungi, C.; Tefera, T. Assessment of Quantitative and Qualitative Losses of Stored Grains Due to Insect Infestation in Ethiopia. *J. Stored Prod. Res.* **2020**, *89*, 101689. [CrossRef]
4. Kumar, D.; Kalita, P. Reducing Postharvest Losses during Storage of Grain Crops to Strengthen Food Security in Developing Countries. *Foods* **2017**, *6*, 8. [CrossRef] [PubMed]
5. Păun, A.; Stroescu, G.; Zaica, A.; Yasbeck Khozamy, S.; Zaica, A.; Cristea, O.; Ştefan, V.; Bălţatu, C. Storage of Grains and Technical Plants through Active Ventilation for the Purpose of Maintaining the Quality of Stored Products. *E3S Web Conf.* **2021**, *286*, 03010. [CrossRef]
6. Chen, C.; Shu, X.; Mo, T.; Li, W.; Zang, C.; Chen, Z.; Wang, Y. A Context Model for Mechanical Ventilation in Grain Storage. In Proceedings of the 2016 9th International Conference on Service Science (ICSS), Chongqing, China, 15–16 October 2016; pp. 88–93. [CrossRef]
7. Agrafioti, P.; Kaloudis, E.; Bantas, S.; Sotiroudas, V.; Athanassiou, C.G. Modeling the Distribution of Phosphine and Insect Mortality in Cylindrical Grain Silos with Computational Fluid Dynamics: Validation with Field Trials. *Comput. Electron. Agric.* **2020**, *173*, 105383. [CrossRef]
8. Ingegno, B.L.; Tavella, L. Ozone Gas Treatment against Three Main Pests of Stored Products by Combination of Different Application Parameters. *J. Stored Prod. Res.* **2022**, *95*, 101902. [CrossRef]
9. Pandiselvam, R.; Chandrasekar, V.; Thirupathi, V. Numerical Simulation of Ozone Concentration Profile and Flow Characteristics in Paddy Bulks. *Pest Manag. Sci.* **2017**, *73*, 1698–1702. [CrossRef]
10. Hammami, F.; Ben Mabrouk, S.; Mami, A. Modelling and Simulation of Heat Exchange and Moisture Content in a Cereal Storage Silo. *Math. Comput. Model. Dyn. Syst.* **2016**, *22*, 207–220. [CrossRef]
11. Chen, Y.; Li, X.; Du, X. Thermal Performance of Double-Skin Roof with Inclined Upper Plate for Grain Depot: Modeling and Experimental Investigation. *Buildings* **2023**, *13*, 2672. [CrossRef]
12. Li, X.; Wang, Y.; Yang, K.; Du, X. Numerical Study of Heat and Mass Transfer during Drying Process of Barley Grain Piles Based on the Pore Scale. *J. Food Process Eng.* **2023**, *46*, e14433. [CrossRef]
13. Li, X.; Yang, K.; Wang, Y.; DU, X. Simulation Study on Coupled Heat and Moisture Transfer in Grain Drying Process Based on Discrete Element and Finite Element Method. *Dry. Technol.* **2023**, *41*, 2027–2041. [CrossRef]
14. Thorpe, G.R. Modelling Ecosystems in Ventilated Conical Bottomed Farm Grain Silos. *Ecol. Model.* **1997**, *94*, 255–286. [CrossRef]
15. Bonjour, E.L.; Opit, G.P.; Hardin, J.; Jones, C.L.; Payton, M.E.; Beeby, R.L. Efficacy of Ozone Fumigation Against the Major Grain Pests in Stored Wheat. *J. Econ. Entomol.* **2011**, *104*, 308–316. [CrossRef] [PubMed]
16. Wang, T.C.; Qu, G.; Li, J.; Lu, N. Transport Characteristics of Gas Phase Ozone in Soil during Soil Remediation by Pulsed Discharge Plasma. *Vacuum* **2014**, *101*, 86–91. [CrossRef]

17. Silva, M.V.A.; Faroni, L.R.A.; Martins, M.A.; Sousa, A.H.; Bustos-Vanegas, J.D. CFD Simulation of Ozone Gas Flow for Controlling Sitophilus Zeamais in Rice Grains. *J. Stored Prod. Res.* **2020**, *88*, 101675. [CrossRef]
18. Mahroof, R.M.; Amoah, B.A.; Wrighton, J. Efficacy of Ozone Against the Life Stages of Oryzaephilus Mercator (Coleoptera: Silvanidae). *J. Econ. Entomol.* **2018**, *111*, 470–481. [CrossRef] [PubMed]
19. Yang, K.; Wang, Y.; Mao, Y.; Zhang, W. Heat and Moisture Transfer in a Rectangular Cavity Partially Filled with Hygroscopic Porous Media. *Heat Transf. Eng.* **2020**, *41*, 814–824. [CrossRef]
20. Veršić, Z.; Binički, M.; Nosil Mešić, M.; Galić, J. Passively Maintained Closed Cavity Façade—Experimental Validation of the Mathematical Thermal Model. *Buildings* **2023**, *13*, 2031. [CrossRef]
21. Fang, Z.; Wang, W.; Chen, Y.; Song, J. Structural and Heat Transfer Model Analysis of Wall-Mounted Solar Chimney Inlets and Outlets in Single-Story Buildings. *Buildings* **2022**, *12*, 1790. [CrossRef]
22. Singh, A.; Gupta, O.P.; Pandey, V.; Ram, S.; Kumar, S.; Singh, G.P. Physicochemical Components of Wheat Grain Quality and Advances in Their Testing Methods. In *New Horizons in Wheat and Barley Research: Global Trends, Breeding and Quality Enhancement*; Kashyap, P.L., Gupta, V., Prakash Gupta, O., Sendhil, R., Gopalareddy, K., Jasrotia, P., Singh, G.P., Eds.; Springer: Singapore, 2022; pp. 741–757. [CrossRef]
23. Balduzzi, F.; Bianchini, A.; Ferrara, G.; Ferrari, L. Dimensionless Numbers for the Assessment of Mesh and Timestep Requirements in CFD Simulations of Darrieus Wind Turbines. *Energy* **2016**, *97*, 246–261. [CrossRef]
24. Isikber, A.A.; Athanassiou, C.G. The Use of Ozone Gas for the Control of Insects and Micro-Organisms in Stored Products. *J. Stored Prod. Res.* **2015**, *64*, 139–145. [CrossRef]
25. Frei, M.; Kohno, Y.; Tietze, S.; Jekle, M.; Hussein, M.A.; Becker, T.; Becker, K. The Response of Rice Grain Quality to Ozone Exposure during Growth Depends on Ozone Level and Genotype. *Environ. Pollut.* **2012**, *163*, 199–206. [CrossRef] [PubMed]
26. Zhang, J.; Wei, Y.; Fang, Z. Ozone Pollution: A Major Health Hazard Worldwide. *Front. Immunol.* **2019**, *10*, 2518. [CrossRef]
27. Van, D.T.H.; Ishii, S.; Oanh, N.T.K. Assessment of Ozone Effects on Local Rice Cultivar by Portable Ozone Fumigation System in Hanoi, Vietnam. *Environ. Monit. Assess.* **2009**, *155*, 569–580. [CrossRef]